Near-field Aerial Overpressure and Impulse from Small-scale BLEVE

El Mehdi Laamarti, A.M. Birk, Frederic Heymes

Near-field Aerial Overpressure and Impulse from Small-scale BLEVE

E.M. Laamarti [a,b], A.M.Birk [a] & F.Heymes[b]

[a] Queen's University Department of Mechanical and Materials Engineering, Kingston ON Canada K7L 3N6

[b] Laboratoire des Sciences des Risques, IMT Mines Ales, Ales, France

E-mail: frederic.heymes@mines-ales.fr

Abstract

This paper presents an investigation into one of the most damaging hazards associated with Boiling Liquid Expanding Vapor Explosion (BLEVE), specifically focusing on the near-field overpressure and impulse effects. Experiments were conducted at a small-scale to study the overpressure and impulse using aluminum tubes with a diameter of 50 mm and a length of 300 mm. The tubes were filled with pure propane liquid and vapor. The controlled variables, on this work included the failure pressure, the liquid fill level, and the weakened length along the tube top. These variables control the strength of the overpressure that is characterized by the peak overpressure amplitude, duration of this overpressure event and the resultant impulse. Notably, these experiments at a small scale included experiments with 100 % liquid fill level. This provided further confirmation that the vapor space is the main driver of the lead overpressure hazard. High speed cameras and blast gauges effectively illustrated the progressive formation of the shock wave in both temporal and spatial dimensions. Furthermore, various predictive models available in the literature are discussed in this paper and new correlations were developed to quantify the overpressure duration and impulse. The current analysis aims to predict the potential consequence of overpressure events during a BLEVE.

Keywords: *Overpressure, Shock wave, Impulse, Propane, Boiling liquid expanding vapor explosion, BLEVE , Vessel failure, Liquid full.*

Introduction

The boiling liquid expanding vapor explosion (BLEVE) constitutes a distinctive form of physical explosion involving a pressure liquefied gas (PLG). It can happen when the pressure vessel containing the PLG is severely weakened by some process such as fire heating. Not all explosions observed fall under the BLEVE classification as it requires rapid total loss of containment (i.e., full opening of the vessel) as proposed by Birk et al. (2007). The BLEVE happens during the sudden explosive release of the vapor and liquid energy upon rapid opening of the vessel. The BLEVE results in rapidly expanding vapor and flashing liquid that will generate hazards including projectiles, fireballs if the commodity is flammable, toxic, or flammable vapor clouds, ground loading, and blast overpressures. These hazards close to urban areas, can cause significant consequences in terms of material losses and human casualties.

Numerous researchers have devised models aimed at facilitating hazard mitigation and prediction. Casal and Salla, (2006); Planas-Cuchi et al. (2004) developed models based on expansion energy using flash fraction of the liquid to quantify the lead shock overpressure. Birk et al. (1996) in response to risk and prevention, developed a model to predict the fireball diameter and duration. Moreover, Baum et al. (2005) established correlations to predict the projectiles velocity and radius of action based on the isentropic expansion energy. As for the ground load, Laamarti E.M. et al. (2024) formulated correlations for estimating peak ground load variables associated with small-scale BLEVE events. The present study focuses on the near-field overpressure and impulse.

Overpressures are produced by the expanding vapor and the flashing liquid. They manifest as waves that propagate over finite distances, yet they possess sufficient strength to induce structural damage to buildings, fracture surrounding glass, and even initiate a cascading chain reaction. Birk et al. (2007) identified three overpressures from a BLEVE. The first two are produced primarily by the vapor space

release and the third by both vapor phase and flashing liquid. The first overpressure is a steep shockwave, followed by a negative phase rarefaction wave caused by the overexpansion of the vapor space. The overexpansion leads to a second weaker shock wave. The third wave is produced by the flashing liquid and is not a shock wave. The prediction of this specific hazard has been extensively explored experimentally and numerically by several authors.

The exact nature of whether the shock wave overpressure results exclusively from vapor and liquid remains a subject to controversy. Giesbrecht et al. (1981) conducted experiments involving rapid catastrophic failure of fully propylene filled glass spheres, showing the generation of an overpressure wave. However, it is not clear if this overpressure was a shock wave (supersonic). Consequently, definitive conclusions regarding the role of liquid phase in shockwave formation remain elusive.

Van der Berg et al. (2004-2005) formulated a one-dimensional expansion-controlled model assuming that flash fraction of the liquid contributes to shock formation. While this assumption leans towards a conservative approach, its accuracy remains uncertain. This perspective contrasted with Baker et al. (1983) that suggested that BLEVE shock formation is only a result of vapor expansion as the liquid flashing is too slow to produce a shock wave. Presently, advancements in data acquisition technologies are leaning toward the understanding that the primary shockwave from BLEVE, is an outcome of the vapor expansion alone, with no significant contribution from liquid phase. The liquid produces a slower and powerful contribution in the form of ground loading, projectiles, and dynamic pressure (drag) effects. Across different scales, Birk et al. (2007), Eyssette (2018) and current experiments provided experimental evidence on contributions of vapor and liquid to BLEVE hazards.

Currently, to estimate the overpressure theoretically, a predominant approach has been based on isentropic expansion energy derived from thermodynamic first principles. Researchers like Brode et al. (1959), and Prugh et al (1991) adopted this method. In contrast, some other models integrated irreversibly to account for heat losses as the one developed by Planas-Cuchi et al. (2004) and Casal et al. (2006). While both approaches yielded conclusive results when compared to experiments, these models, while informative, fail to account for the complexity of opening dynamics in real-world scenarios and do consider flash fraction of the liquid in shock formation. Nevertheless, a new approach, far from energy models, was introduced by Birk et al. (2018) with the shock start model using the 1D shock tube equation and spherical shock wave theory.

This paper presents a set of new overpressure data from 2022 experimental campaign done by Laamarti E.M. et al. (2024) complemented by data from Eyssette (2018). The collected data include a broader range of controlled variables, including failure pressure, liquid fill level and weakened length, thereby extending the scope of the existing data. Notably, analysis on unaddressed aspects of overpressure was carried out using all the experimental results from a small-scale apparatus. This study further investigates the use of Friedman-Whitham approach for spherical shock waves combined with the shock tube model. Correlations are introduced to address the interplay of dependent overpressure variables, specifically the lead overpressure peak and duration, and the resulting impulse.

1. Small scale propane BLEVE experiments

1.1. Experimental apparatus

The experiments were conducted with small-scale tubes of 300 mm length and 50 mm diameter. A total of 36 experiments were conducted in 2022. The tubes were made from aluminum type 6061 T6 annealed to T0 temper to reduce the material's yield and ultimate strength. The tubes were machined along the top to reduce the wall thickness along a defined weakened length. To reduce the effects of age hardening, the tubes were stored in a freezer at -40ºC before the testing. The tube preparation facilitated tube rupture at desired failure pressures, thereby delineating both the location and size of the burst opening. To initiate the BLEVE, the tubes were filled with propane and subjected to an external heater, along the tube bottom (Fig.1.[Left]). The heater primarily heated the liquid to produce saturated mixture of liquid and vapor. The heating caused the pressure to rise in the vessel until it

failed. Failure occurred in the weakened length when the von Mises stress reached the yield strength of the annealed aluminum. High and low speed instruments were used to capture the hazards produced by the small-scale BLEVE. This included thirteen pencil blast gages positioned at varied locations, diverse angles, and elevations [vertical, horizontal, 45º angle] around the subjected tubes. The vertical gages PCB 137B28 labelled TOP 1,2,3 and 4, are positioned respectively at 15,20,30 and 40 cm above the tube. These gages boast a range of 3.45 bar, a response time of 1 µs, a sensitivity of 14.5mV/kPa and an uncertainty of under 2%. The remaining gages, PCB 137A23, are placed at different angles and sampled at 200 kHz. They also have a range of 3.45 bar, a response time of 4 µs, a sensitivity of 14.5 mV/kPa and an uncertainty of 0.2 %.

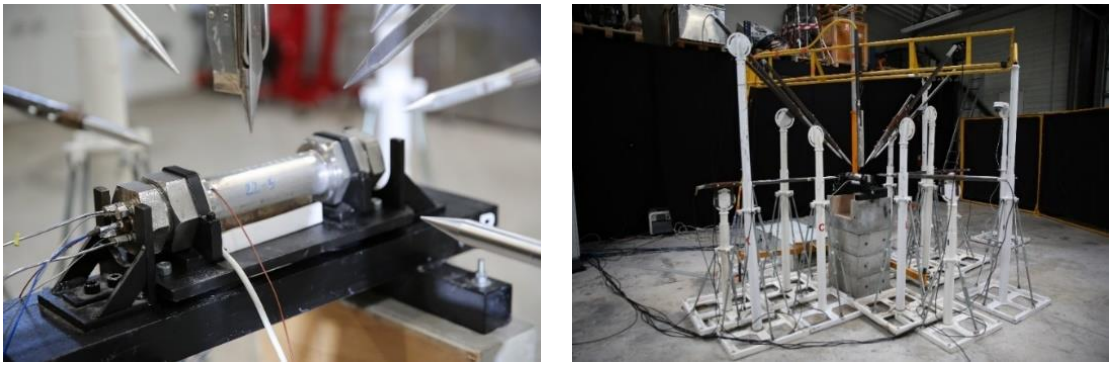

Fig. 1. *BLEVE 2022 Experimental apparatus*

Three high speed cameras were strategically positioned at the front, side, and window views to capture the details of the explosion and observe the overpressure details. Operating at a rate of approximately 24,000 fps, these cameras featured an exposure duration of 40 µs. A detailed description of the apparatus is presented in Laamarti.E.M et al. (2024).

1.2. Experimental apparatus

The small-scale BLEVE experiments carried out in 2022 [Fig.2] by Laamarti.E.M et al. (2024) for various operating conditions has been complemented by data from Eyssette (2018) [Fig.3]. The controlled variables that were selected to attain the desired burst conditions included:

- Failure pressure P_f [Barg or Bara] : g and a stand for gage and absolute pressure
- Liquid fill (volume fraction) φ [%]
- Weakened length L_c [m]

These variations in operating conditions help understand the impact of controlled variables and whether similar conditions can yield to same outcomes.

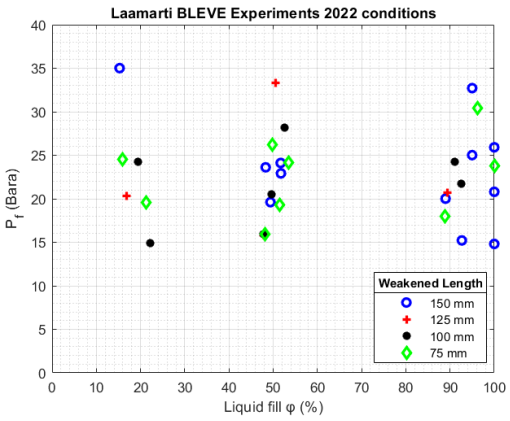

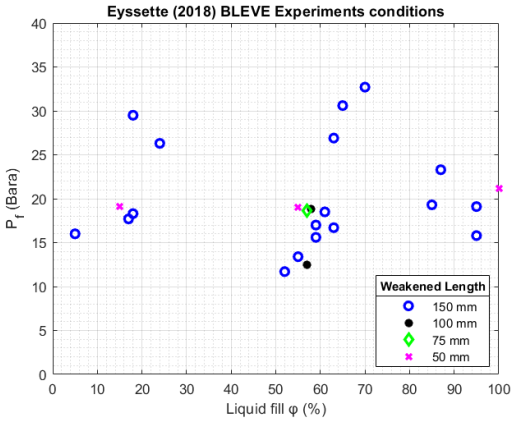

Fig. 2. *Summary Laamarti BLEVE Experiments 2022* ***Fig. 3.*** *Summary Eyssette (2018) BLEVE Experiments*

New data for 100 % liquid fill level was achieved to discern the specific contribution of liquid phase in the formation of shockwaves. The experimental variables were systematically modified in a progressive manner, thereby facilitating an investigation into the individual influence exerted by each

variable on the resultant blast wave. Among the experiments, a total of nine experiments resulted in partial opening of the vessel, thus showing the effect of opening size on the strength of the hazards produced by the BLEVE.

1.3. BLEVE Overpressures

Variations in the operating conditions generate various data on the dependant near-field overpressure variables. Conventionally, a BLEVE produces a sequence of overpressure events, consisting of an initial first lead shock overpressure from vapor phase followed by an under-pressure wave, a second wave from vapor phase and a third wave overpressure from both vapor phase and liquid flashing. Fig.4 shows a typical blast data measured at 20 m from a 2000 L propane tank. Three successive wave overpressures generated during a BLEVE are visible on the graph. The magnitude, the duration and the impulse of the lead shock overpressure will be explored in this study.

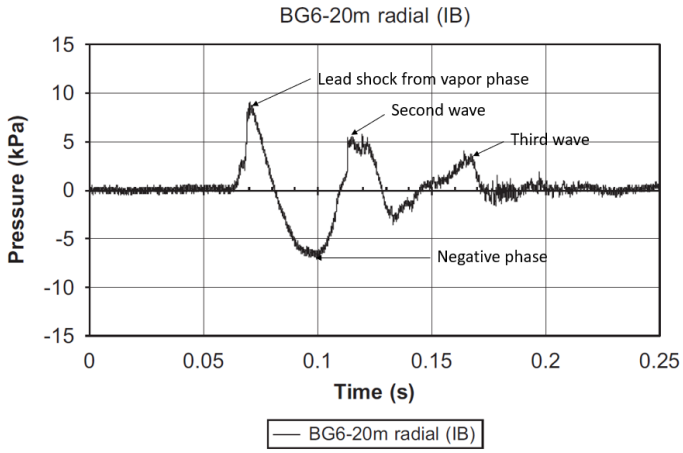

Fig. 4. *Overpressure measured at 20 m from the side of a 2000 L propane tank, Birk et al. (2007)*

The objective is to formulate a physics-based analysis of the dependant variables, specifically extracted from vertical blast gages, because they measured the strongest overpressure for the top opening failure. The variables were:

- Peak overpressure of the first wave [Bar]
- Duration of the first wave overpressure [s]
- Impulse per unit area of the first wave overpressure [Bar.s]

The lead shock decays with distance and is assumed to follow spherical shock theory. The data suggests that vessel filled to 100 % capacity with liquid generate solely an overpressure with no shockwaves. Thus, the shock tube equations and the Friedman-Whitham spherical shock theory cannot be applied.

2. Numerical Methods

2.1. Shock tube theory

During a BLEVE, the pressure vessel fails, and the vapor leaves the vessel, creating pressure on the surrounding air. This rapid pushing on the atmosphere results in a series of compression waves that pile up and forms a supersonic shock wave to meet the flow constraints (Fig.5).
Commonly referred to as a “surface of discontinuity”, the shock wave refers to a sharp pressure rise that then tails off with distance. The shock strength and shape depend on many factors, such as:

- The operating conditions: Failure pressure, weakened length, liquid fill.
- The type of opening: whether partial or full opening of the pressure vessel.
- The rate of opening due to the uneven thickness of the weakened length

The BLEVE resulting from a cylindrical vessel will generate a cylindrical shock that will transition to a spherical shock as it propagates through an unconfined environment at a transient state. The

initial overpressure can be calculated using the shock tube equation, especially if the opening of the vessel is extremely rapid. To use the normal shock tube equations and accurately determine the stagnation properties, it is essential to transition from the unsteady moving normal shock resulting from the explosion to a steady state by moving with the shock [Fig.5].

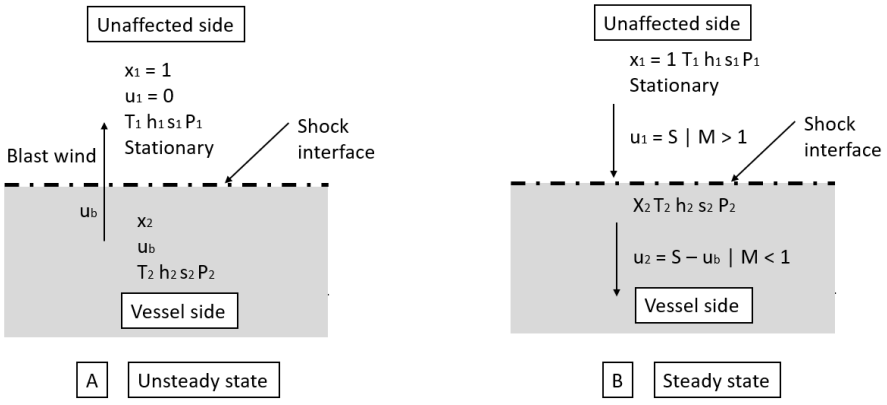

Fig. 5. *Shock wave for [A] unsteady and [B] steady cases*

The 1D normal shock tube equations developed by Rankine-Hugoniot (1870) can then be applied to address the stationary problem. These equations satisfy the continuity, momentum and energy equations which result in:

$$\frac{P_4}{P_1} = \frac{P_2}{P_1}\left[1 - \frac{(\gamma_4 - 1)\frac{a_1}{a_4}(\frac{P_2}{P_1} - 1)}{\sqrt{2\gamma_1(2\gamma_1 + (\gamma_1 + 1)(\frac{P_2}{P_1} - 1)}}\right]^{\frac{-2\gamma_4}{\gamma_4 - 1}} \quad (1)$$

The static pressures obtained by transitioning to steady state are: (White,1986):

$$\frac{P_2}{P_1} = \frac{2\gamma_1 M^2}{(\gamma_1 + 1)} - \frac{(\gamma_1 - 1)}{(\gamma_1 + 1)} \quad (2)$$

$$\Delta p_{st} = (P_2 - P_1) => overpressure \quad (3)$$

- *State 2:* Explosion side (before shock = downstream part)
- *State 1:* Unaffected side (after shock = upstream part) at ambient conditions

h_1 and h_2: Enthalpy at state 1 and 2
T_1 and T_2: Static temperature at state 1 and 2
P_1 and P_2: Static pressure at state 1 and 2
S_1 and S_2: Entropy at state 1 and 2
γ_4: Propane specific heat ratio (1.3)
u_b: Blast wind speed (speed of air behind the shock)
S: Supersonic shock speed
P_4: Static failure pressure
γ_1: Air specific heat ratio (1.4)
a_4: Speed of sound in propane
M: Mach number
a_1: Speed of sound in air

All terms are expressed in SI units : meters (m), seconds (s), pascals (Pa), Joule (J), Kelvin (K).

2.2. Friedman Whitham approach

Under the assumption of spherical expansion, the variation of shock strength with distance can be predicted using the Friedman Whitham relation (Friedman,1960) as follows:

$$\left[\frac{\boldsymbol{R}}{\boldsymbol{R_0}}\right]^{\mathbf{2}} = \boldsymbol{e}^{(2\gamma_1 - 2)^{-\frac{1}{2}}} \mathbf{sin}^{-\mathbf{1}}\left[\frac{\mathbf{2}\boldsymbol{Y}^{\mathbf{2}} - (\boldsymbol{\gamma_1} - \mathbf{1})\boldsymbol{Z}^{\mathbf{2}}}{(\boldsymbol{\gamma_1} + \mathbf{1})^{\mathbf{2}}\boldsymbol{M}^{\mathbf{2}}}\right] \quad (4)$$

Where

$$Y = (2\gamma_1 M^2 - \gamma_1 + 1)^{\frac{1}{2}} \quad (5)$$

$$Z = ((\gamma_1 - 1)M^2 + 2)^{\frac{1}{2}} \quad (6)$$

$$W = \frac{(Y-Z)^2}{M}\left[Y(\gamma_1-1)^{\frac{1}{2}} + Z(2\gamma_1)^{\frac{1}{2}}\right]^{\left(\frac{2\gamma_1}{\gamma_1-1}\right)^{\frac{1}{2}}} Y^{\frac{2}{\gamma_1}} \quad (7)$$

R: Radius of the hemispherical shock

R_0: Radius of the hemispherical sphere surface of the vapour phase where the shock started

$$R_0 = \left[\frac{3(1-\varphi)}{4\pi}\frac{V_{tube}}{2}\right]^{\frac{1}{3}} \quad (8)$$

V_{tube}: Volume of the tube

$$\left[\frac{\Delta p_{exp}}{\Delta p_{st}}\right] = \left[\frac{R}{R_0}\right]^n \simeq \left[\frac{\Delta p_{Fw}}{\Delta p_{st}}\right] = \left[\frac{R}{R_0}\right]^n \quad (9)$$

Δp_{Fw} : Overpressure from Friedman Whitham

Δp_{exp}: Experimental overpressure

Δp_{st} : Overpressure from shock tube equations

n: Index

2.3. Duration of lead overpressure

The duration of the lead overpressure is an important dependant variable that helps evaluate the strength of the shock. The longer the duration of lead overpressure prolongs the exposure of structures to the intense force exerted by the blast wave potentially leading to great damage. Moreover, prolonged overpressure can result in secondary effects such as structural fatigue and domino effects. The experimental value is found from the base of the triangular shaped peak overpressure. The duration of lead overpressure, being solely an outcome of the vapor phase, can be rendered non-dimensional by dividing it by the duration of vapor release.

$$t^*_{ov} = \frac{t_{ov}}{t_{vap}} \quad with \ t_{vap} = \frac{D}{a} \quad (10)$$

t_{ov} : Experimental duration of overpressure [s]

D : Tube diameter [m]

t^*_{ov}: Dimensionless duration of overpressure

t_{vap}: Duration of the vapor phase [s]

a : Speed of sound in vapor propane [m/s].

2.4. Impulse per unit Area

The impulse per unit area is determined by integrating the first peak overpressure over its duration. The wave form is nearly an isosceles triangle, and the integral is approximately equal to :

$$I_{ov} = \frac{\Delta p_{exp}\, t_{ov}}{2} \quad (11)$$

I_{ov} : Experimental Impulse per unit area [bar. s]

The formula corresponds to the impulse per unit area experienced by an object exposed to a blast. The condition is that the object is small enough for the impulse per unit area to remain constant across its surface.

2.5. Correlation equation

The duration and the impulse from the first overpressure have been correlated to the independent variables to formulate a predictive equation equal to:

$$t^*_{ov} = \frac{t_{ov}}{t_{vap}} \qquad \frac{t_{ov\_cor}}{t_{vap}} = t^*_{ov\_cor} = K_1\left(\frac{P_f}{P_{atm}}\right)^a (\varphi)^b \left(\frac{L_c}{L_v}\right)^c$$

$$t_{ov} \simeq t_{ov\_cor} = K_1\left(\frac{P_f}{P_{atm}}\right)^a (\varphi)^b \left(\frac{L_c}{L_v}\right)^c t_{vap} \quad (12)$$

t_{ov_cor}: Correlated duration of lead overpressure [s]

a, b. c, K_1, are constants

For the impulse per unit area, and the corresponding equation is :

$$I_{ov\_cor} = \frac{\Delta p_{Fw}\, t_{ov\_cor}}{2} \tag{13}$$

3. Results and discussion

3.1. Opening dynamics

The opening dynamics of the vessel are believed to strongly influence the resultant overpressure. Experiment 30 from Laamarti BLEVE experiments 2022 can be compared with Experiment 26 by Eyssette (2018) under similar initial conditions of failure pressure, liquid fill and weakened length. Fig.6 [Left] shows the lead overpressures and Fig.6 [Right] shows the tube opening. As it can be seen, the overpressure vs time is quite similar except the Eyssette (2018) data shows a rising pressure after the initial overpressure. This could be attributed to the larger size of the laboratory used in the Eyssette (2018) experimental campaign and the difference of 5-10 % liquid fill, which couldn't be precisely controlled due to leaking issues.

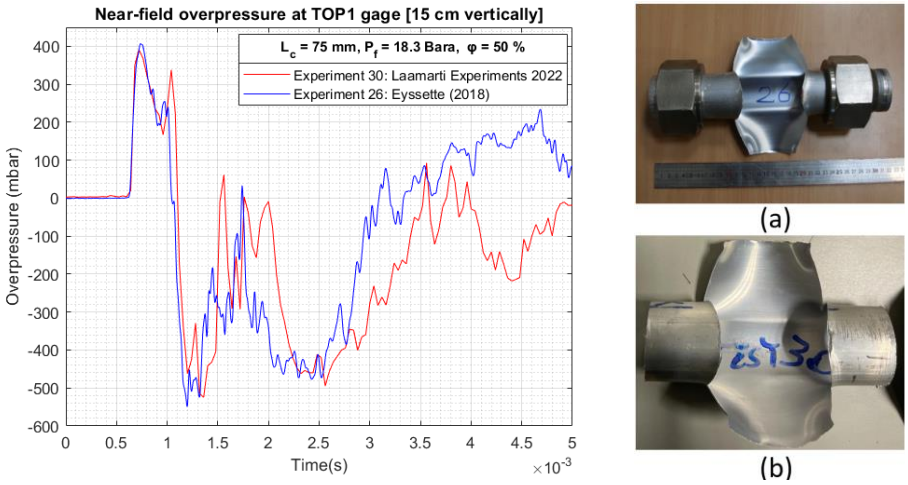

Fig. 6. *Lead overpressure TOP 1 vertical gage (15cm) [a] Eyssette (2018) [b] Laamarti Experiments 2022*

3.2. Influence of failure conditions on top vertical blast overpressure

The controlled failure conditions influence the lead overpressure strength and impulse. While prior studies on near field overpressure predominantly focused on the blast wave's peak overpressure, this investigation extends its scope to include the study of the impulse. To discern the impact of the controlled variables, experiments were selected with similar conditions and with only one parameter changing at a time (Fig.7).

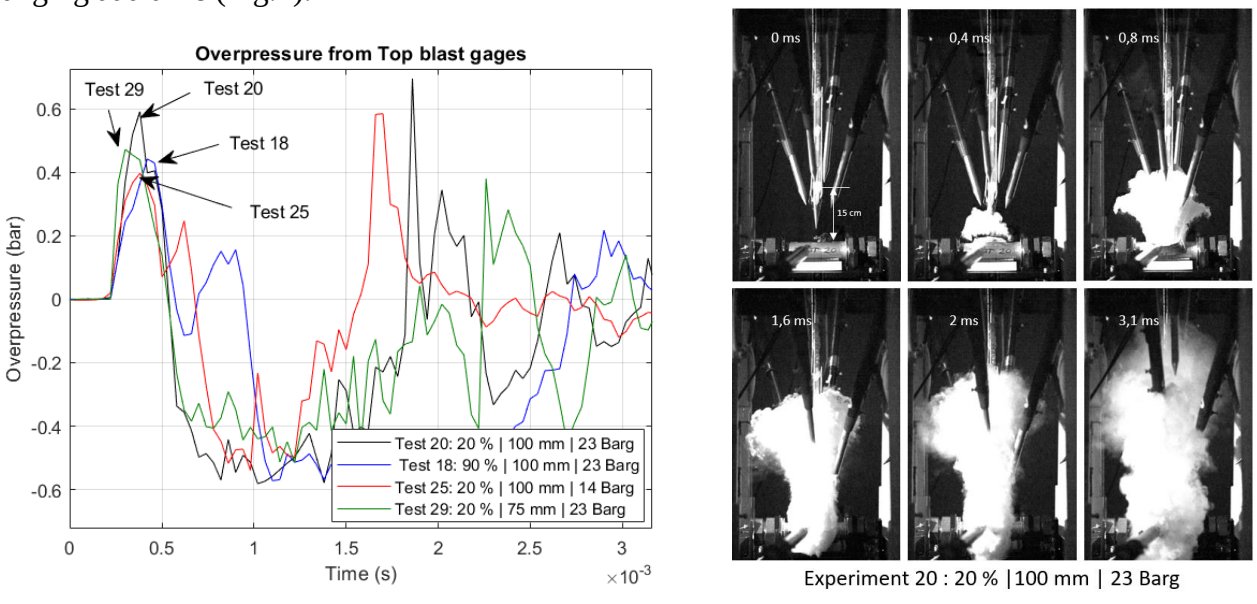

Fig. 7. *[Left]Comparative study of the first lead peak overpressure from TOP 1 blast gage [Right]High-speed camera Experiment 20; Frame 1 (time =0 ms): no failure, Frame 2 (time = 0.4 ms): Lead shock reached TOP 1 (15 cm), small white cloud (vapour) starting. Frame 3 (time = 0.8-1.2 ms): Flashing process. Horned beast expansion of contents. Frame 4-5 (time = 1.6-2 ms): Internal vessel pressure drops progressively to atmospheric pressure and the second wave reaches TOP 1 gage. Frame 6 (time = 3.1=5.2 ms): Cloud dispersion*

The sequence of events remains consistent across the experiments; however, the duration of these events varies depending on the operating conditions and the opening dynamics involved.
Using experiment 20 as a reference point, experiments 18, 25 and 29 respectively represent an increase of liquid fill, a decrease of failure pressure and a decrease of weakened length. Fig.7a shows the overpressures measured by the blast sensor TOP 1 positioned 15 cm above the top of the tube. Below are summaries of the experiments.

Experiment 20 \Experiment 18: Increase of the liquid fill level from 20 % to 90 %

- reduced maximum peak overpressure.
- increased duration of the peak wave.
- reduced impulse.
- formed two clear pressure peaks.
- negative phase amplitude is similar for both experiments.

In fact, high liquid fill level does imply lower amount of vapor phase energy and thus a more rapid decay of overpressure with distance.

Experiment 20 \ Experiment 25: Decrease of the failure pressure from 23 to 14 Barg.

- reduced maximum peak overpressure.
- increased duration of the peak wave
- reduced impulse.
- reduced the negative phase amplitude.
- ratio of failure pressures is equal to the ratio of peak overpressures (0.67)

The failure pressure describes the pressure difference between the atmospheric pressure and the tube pressure. As expected, lower failure pressure produces a weaker pressure wave.

Experiment 20 \ Experiment 29: Decrease of the weakened length from 100 to 75 mm.

- smaller opening
- reduced maximum peak overpressure.
- no change on duration of peak wave
- slightly reduced the negative phase amplitude.

The contents exiting the pressure vessel through a smaller opening area had an impact on the maximum peak overpressure, as the reduced opening of the vessel walls interfered with the formation of the shock.
Overall, it was observed that all controlled operating conditions resulted in changes to the overpressure characteristics measured at 15 cm above the tube. An important dependence was noted for failure pressure and liquid fill level, while a partial dependency was identified for weakened length. This underscores the necessity to develop correlations that link lead overpressure characteristics to the controlled variables. While the crack velocity, which describes the way the pressure vessel opens, is believed to exert a certain impact, control over this parameter has not been achieved to date.

3.3. Estimation of the lead peak overpressure

The lead peak overpressure from the vertical blast gage at 15 cm above the tube is presented in Fig. 8 and 9 for both Laamarti BLEVE 2022 campaign and Eyssette (2018) as a function of the failure pressure, liquid fill, and weakened length. The graphical representations reveal a discernible pattern: the magnitude of the experimental overpressure consistently increases with an increase in failure pressure and weakened length, while it decreases with a rise in liquid fill. This phenomenon can be attributed to the vapor phase; a larger volume of vapor phase correlates to a slower pressure decay over distance, resulting in a higher magnitude of overpressure at a specified distance. Moreover, the graph shows that at a similar failure pressure, the 100 % liquid fill cases failed partially and gave the lowest peak overpressure.

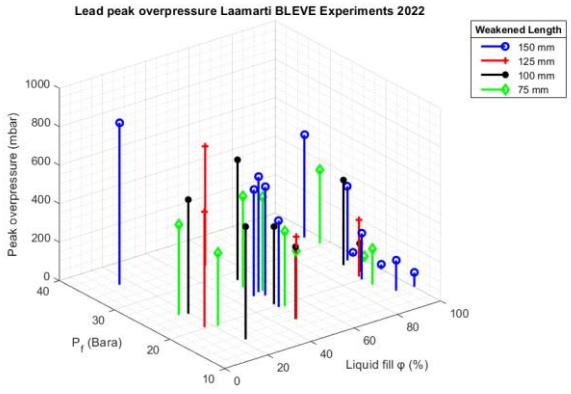

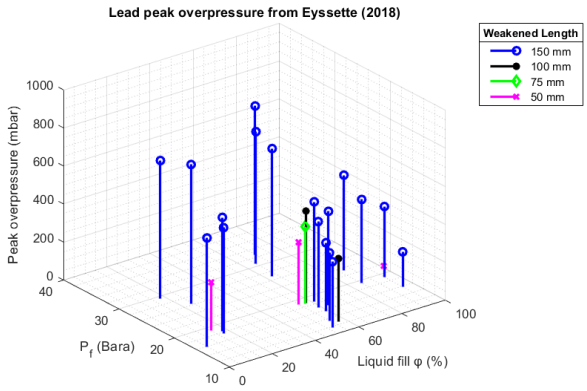

Fig. 8. *Lead peak overpressure Laamarti Experiments 2022* ***Fig. 9.*** *Lead peak overpressure Eyssette (2018)*

The experimental peak overpressures were normalized by the calculated peak overpressures from the shock tube equation under identical operating conditions. These normalized values are represented in Fig.10 with respect to dimensionless distance.

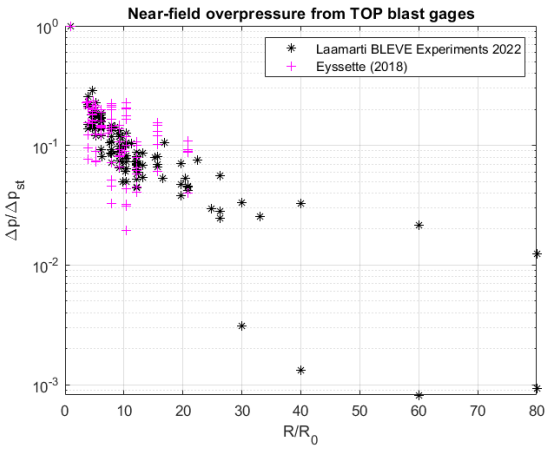

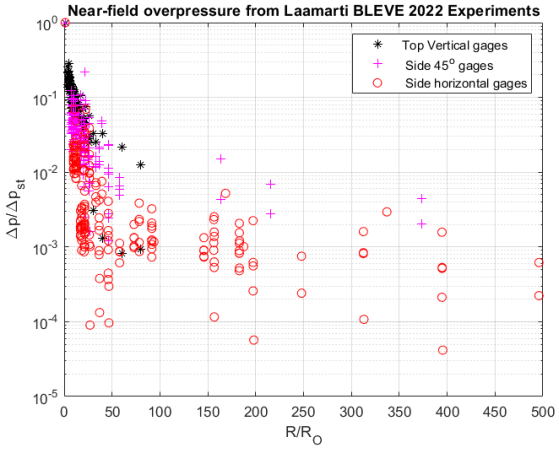

Fig. 10. *Lead peak overpressure from TOP blast gages* ***Fig. 11.*** *Lead peak overpressure from all gages*

Results from both campaign exhibit similarities, overlaying each other and revealing the general behaviour of the shock wave. As distance increases, the overpressure shows a 1/R rate of decay, indicative of the weakening shock because of energy dissipation in the surrounding atmosphere and an expanding shock surface area. Experimental findings demonstrate that the vertical overpressures are more powerful compared to those measured by the 45º angle gages and the horizontal gages, as depicted in Fig.11. This can be primarily attributed to the dynamics of opening, particularly the energy required to flatten the vessel walls.

The experimental findings presented above can then be contrasted with the prediction from the Friedman-Whitham theory for each experiment, for instance experiment 2 and 6 are illustrated in Fig. 12. The overpressures were normalized by the overpressure from the shock tube equations.

The comparison between experiments and the Friedman Whitham approach for experiment 2 indicates a good approximation of the solution with a minor discrepancy observed in the exponent value. This deviation in results can be attributed to small differences in the opening of the vessel. For lower liquid fill levels, the overpressures are faster and stronger and the Friedman-Whitham model tends to overpredict the actual experimental data. Furthermore, the shock fully forms within the 3-4 times the tube diameter range, thus it may fully form at TOP 2, 20 cm above the tube, rather than TOP 1 (15 cm). This is visible for experiment 6 where the second experimental overpressure data point at 20 cm surpasses the first one at 15 cm.

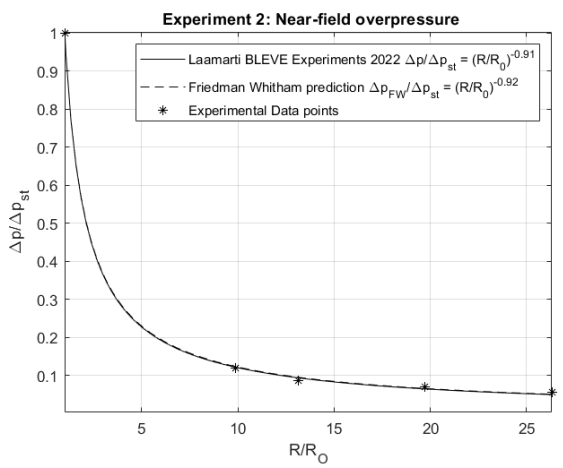

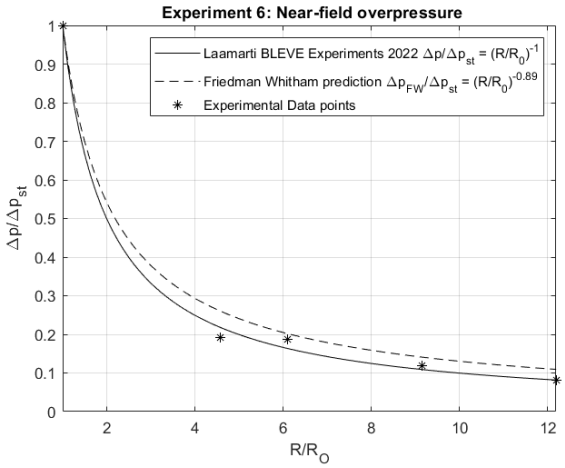

Experiment 2: 99 % | 150 mm | 24 Barg **Experiment 6:** 50 % | 150 mm | 23.1 Barg

Fig. 12. *Comparative study of the prediction of the overpressure from blast vertical top gages*

The Friedman-Whitham prediction is compared with the experimental overpressure data obtained for all experiments at various heights above the tube as illustrated in Fig.13.

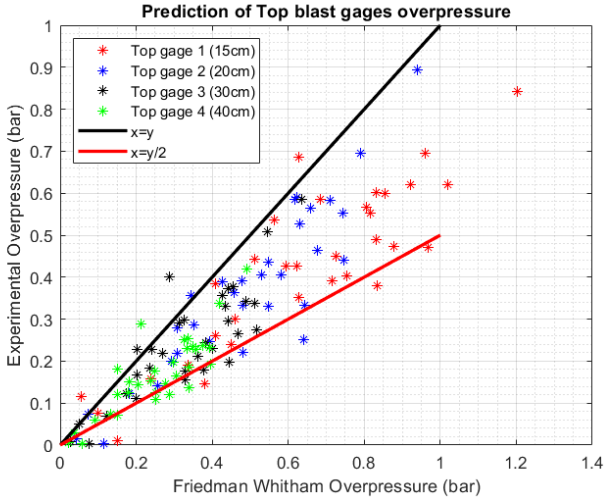

Fig. 13. *Comparative study of the prediction of the overpressure from blast TOP gages*

The graph distinctly illustrates that the Friedman-Whitham relation tends to slightly overestimate the experimental overpressure. However, it is noteworthy that dividing the Friedman-Whitham formula by approximately half underestimate the weakest overpressures.

On the overall experiments, the exponent for vertical blast gages was obtained between -0.8 and -1.02 for the Friedman-Whitham approach and between -0.87 to -1.25 for the experiments such as:

$$\left[\frac{\Delta p_{exp}}{\Delta p_{st}}\right] = \left[\frac{R}{R_0}\right]^{-0.87\ to -1.25} \simeq \left[\frac{\Delta p_{Fw}}{\Delta p_{st}}\right] = \left[\frac{R}{R_0}\right]^{-0.8\ to -1.02}$$

3.4. Estimation of the duration of lead overpressure

The power of a shock aligns with the energy of the overpressure over time – indicating that a longer duration of overpressure corresponds to a stronger shock. Thus, this investigation targets the duration of overpressure quantified by measuring the integral under the maximum peak overpressure, evenly distributed along the isosceles triangle. Fig.14 illustrates the overpressure duration under various operating conditions derived from 2022 and Eyssette (2018) experimental campaigns. In Fig.14, it is observed that the experimental duration of lead overpressure increases with higher liquid fill. Conversely, an increase in failure pressure leads to a decrease in experimental duration. The influence

of weakened length is less evident. Importantly, cases with 100 % liquid fill showed the longest duration of lead overpressure.

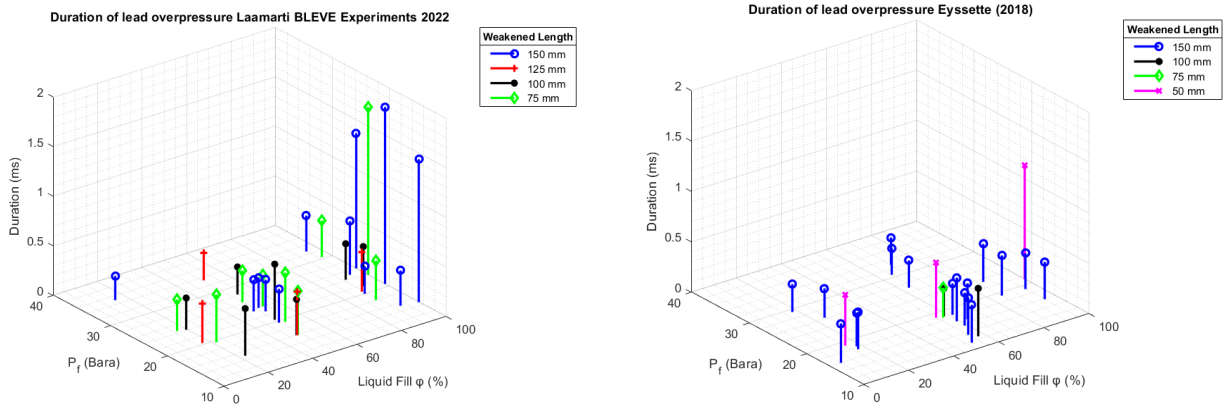

Fig. 14. *Duration of TOP 1 gage [15cm] lead overpressure from [Left] BLEVE 2022 [Right] Eyssette(2018)*

The dimensionless duration of lead overpressure [Equation 10] has been calculated for both Laamarti BLEVE 2022 experiments and Eyssette (2018). A correlation [Equation 12] with specific exponents has been numerically derived to match the dimensionless duration from 2022 experimental data based on operating conditions. Subsequently, this correlation has been then applied to Eyssette (2018) experiments, showing a very consistent fit with the results ($y = x^{0.99}$). Fig. 15 [Left] shows the dimensionless duration of overpressure with respect to the correlation for both campaigns.

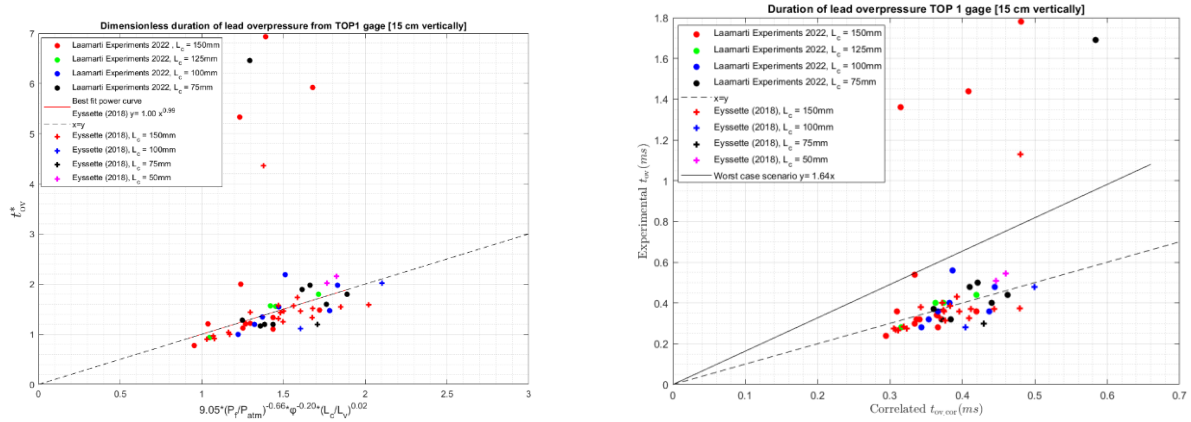

Fig. 15. [Left] *Dimensionless duration of lead overpressure at TOP 1 gage (15 cm vertically) [Right] Experimental vs correlated duration of lead overpressure from TOP 1 gage (15 cm vertically)*

The graph reveals five data points with a distinct behaviour from the rest. These points are 100 % liquid fill scenarios, and they have a prolonged duration of lead overpressure compared to other experiments because of the different opening dynamics involved. Consequently, the 100 % liquid fill cases are not included in the formulation of the duration of lead overpressure. The average duration of lead overpressure found numerically is expressed as follows:

$$t_{ov\_cor} = 9.05\left(\frac{P_f}{P_{atm}}\right)^{-0.66} (\varphi)^{-0.20}\left(\frac{L_c}{L_v}\right)^{0.02} t_{vap}$$

Fig. 15 [Right] shows the experimental vs correlated duration of lead overpressure. From the graph, the highest duration covering the upper bound of data cloud (100 % liquid fill excluded) is

$$t_{ov\_cor\_max} = k t_{ov\_cor} \qquad with\ k = 1.64$$

This correlation is applicable within 3-4 times the diameter (3-4D) range, where the maximum peak overpressure was registered, and has undergone validation exclusively at small scale (D = 50 mm L/D = 6) for both Laamarti Experiments 2022 and Eyssette (2018) data. There are not applicable for 100 % liquid fill, and they require validating at larger scale.

3.5. Estimation of the impulse per unit area

The experimental peak overpressure is shown as a function of the lead overpressure duration in Fig. 16 [Left]. The plot shows that the highest peak overpressures have shorter durations. The duration will depend on the weakened length, the failure pressure, the liquid fill, and the opening dynamics. Fig.16. [Left] shows again the five points, each with 100 % liquid fill, as observed in Fig.15. These points exhibit a combination of low overpressure magnitude and long duration, despite having similar failure pressures as the other liquid fill cases. This suggests the distinctive characteristics of BLEVEs with 100 % liquid fill. Further investigation is required for this specific BLEVE scenarios. Fig.16 [Right] shows that most of experimental results lie beneath the average predicted impulse line, aligning with the intended goal of overpredicting the results. The upper and lower bounds of the experimental impulse are determined by twice and one-fourth the average impulse.

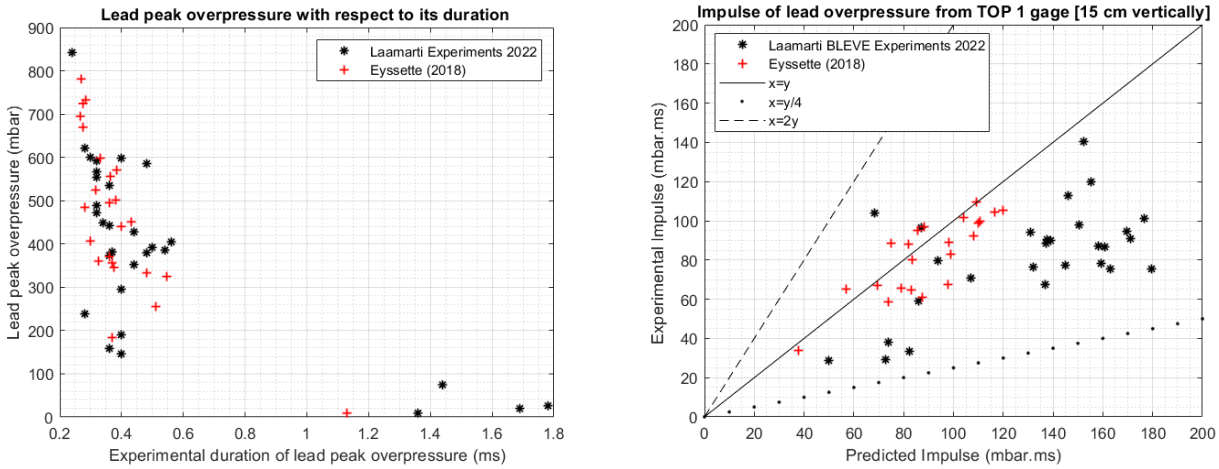

Fig. 16. [Left] Experimental Lead peak overpressure vs overpressure duration [Right] Experimental Impulse per unit area vs Correlated Impulse per unit area.

By employing Equation 13, the correlation for impulse per unit area can be written as:

$$I_{ov\_cor} = \frac{\Delta p_{Fw} 9.06 \left(\frac{P_f}{P_{atm}}\right)^{-0.66} (\varphi)^{-0.20} \left(\frac{L_c}{L_v}\right)^{0.02} t_{vap}}{2}$$

$$I_{ov\_cor} = \frac{\Delta p_{st} \left[\frac{R}{R_0}\right]^{-0.8\ to -1.02} 9.06 \left(\frac{P_f}{P_{atm}}\right)^{-0.66} (\varphi)^{-0.20} \left(\frac{L_c}{L_v}\right)^{0.02} t_{vap}}{2}$$

4. Conclusion

The investigation into near-field overpressure from small-scale propane BLEVE experiments (D = 50 mm, L = 300 mm, volume =589 cm^3) provides new insights into the calculation of impulse per unit area from the lead blast overpressure. The study focused on vertical blast gages positioned above the tube, precisely where the maximum peak overpressure is registered.

Analysis of the Laamarti BLEVE experiments 2022 and Eyssette (2018) experimental campaign revealed that experiments with high failure pressures, low liquid fill levels, and long weakened lengths produced the highest peak overpressures. Notably, experiment 16 from BLEVE experiments 2022 exhibited the greatest peak overpressure, aligning with the highest failure pressure (35 Barg), the longest weakened length (150 mm), and the lowest liquid fill level (15 %). This observation suggests that the vapor phase contributes to high overpressure magnitude and is mainly responsible for shock formation.

The duration of lead overpressure was found to increase with high liquid fill levels and low failure pressures. However, when the liquid fill level reached 100 % (compressed liquid), the duration of lead overpressure was relatively longer. Consequently, the established correlation is not applicable to scenarios involving 100 % liquid fill.

Finally, a formula for the impulse per unit area was derived based on the Friedman-Whitham approach and the developed correlation for the duration of lead overpressure. Presently, this impulse formula

is validated only at a small scale and still require validation at a larger scale. Moreover, it is important to reiterate that the correlation does not apply to liquid full fill cases where the vessel fails under hydrostatic conditions. Hence, additional investigation is necessary for scenarios involving 100 % liquid fill, as they represent a specific case of BLEVE.

Acknowledgements

The authors gratefully acknowledge the financial contribution from Queen's University, Kingston, Canada and IMT mines Ales, Ales, France.

References

Baker, W.E., Cox, P.A., Westine, P.S., Kulesz, J.J., Strehlow, R.A., 1983. Explosion hazards and evaluation. Elsevier Scientific Pub. Co. doi:10.1016/0010-2180(85)90099-9

Baum, H. and Rehm, R. (2005), Simple Model of the World Trade Center Fireball Dynamics., , Chicago, IL, [online], https ://tsapps.nist.gov/publication/getpdf.cfm?pubid = 101087

Birk, A. M. (1996). Hazards from propane BLEVEs: An update and proposal for emergency responders. Journal of Loss Prevention in the Process Industries, 9(2), 173–181.doi:10.1016/0950-4230(95)00046-1

Birk,A.M.,Vandersteen,J.D.J.,2006.On the transition from non BLEVE to BLEVE failure for a1.8 m3propane tank.ASMEJ.Press.VesselTechnol.128(4),648–655.

Birk, A.M., Davison, C., Cunningham, M., 2007. Blast overpressures from medium scale BLEVE tests. J. Loss Prev. Process Ind. 20, 194–206. doi:10.1016/j.jlp.2007.03.001

Birk, A.M., Heymes, F., Eyssette, R., Lauret, P., Aprin, L., Slangen, P., 2018. Near-field BLEVE overpressure effects: the shock start model. Process. Saf. Environ. Prot. 116, 727–736.

Birk, A.M., Eyssette, R., Heymes, F., 2020. Analysis of BLEVE overpressure using spherical shock theory. Process. Saf. Environ. Prot. 134, 108–120.

Brode, H., 1959. Blast Wave from a Spherical Charge. Phys. Fluids 2, 217–229.

Casal, J., Salla, J.M., 2006. Using liquid superheating energy for a quick estimation of overpressure in BLEVEs and similar explosions. J. Hazard. Mater. 137, 1321–1327.
Eyssette, R., 2018. Characterization and modeling of near-field BLEVE overpressure and ground loading hazards. Queen's University (Canada) / IMT Mines Ales (France).

Eyssette, R., Heymes, F., Birk, A.M. "Ground Loading from BLEVE through Small Scale Experiments: Experiments and Results." Process Safety and Environmental Protection, (2021), 148, pp. 1098-1109. doi: 10.1016/j.psep.2021.02.031. [hal-03158570]

Friedman, M P. A SIMPLIFIED DESCRIPTION OF SPHERICAL AND CYLINDRICAL BLAST WAVES. United States: N. p., 1960. Web. doi:10.2172/4115078.

Giesbrecht, H., Hess, K., Leuckel, W. Maurer, B. (1981), 'Analysis of explosion hazards on spontaneous release of inflammable gases into the atmosphere. part1/part2

Laamarti, E.M., Birk, A.M., Chanut, C., Heymes, F., 2024. Correlations to estimate the ground loading from small scale propane BLEVE experiments. Process Safety and Environmental Protection. https://doi.org/10.1016/j.psep.2024.03.006

Laboureur, D., Birk, A.M., Buchlin, J.M., Rambaud, P., Aprin, L., Heymes, F., Osmont, A., 2015. A closer look at BLEVE overpressure. Process Saf. Environ. Prot. 95, 159–171. doi:10.1016/j.psep.2015.03.004

Planas-Cuchi, E., Salla, J.M., Casal, J., 2004. Calculating overpressure from BLEVE explosions. J. Loss Prev. Process Ind. 17, 431–436. doi:10.1016/j.jlp.2004.08.002

Prugh, R.W., 1991. Quantitative Evaluation of Bleve Hazards. J. Fire Prot. Eng. 3, 9–24. doi:10.1177/104239159100300102

Rankine, W. J. M. (1870). "On the thermodynamic theory of waves of finite longitudinal disturbances". Philosophical Transactions of the Royal Society of London. 160: 277–288. doi:10.1098/rstl.1870.0015.

Van den Berg, A., Van der Voort, M., Weerheijm, J., Versloot, N., 2006. BLEVE blast by expansion-controlled evaporation. Process Saf. Prog. 25 (1), 44–51

White, F.M., 1998. Fluid Mechanics, Fourth edition. WCB McGraw-Hill, New York.